Orographic Precipitating Systems

Dr. Yuh-Lang Lin, ylin@cat.edu; http://mesolab.org (or http://mesolab.us)
Department of Physics/AST PhD Program
North Carolina A&T State University
(Ref.: *Mesoscale Dynamics*, Y.-L. Lin, Cambridge, 2007)

Chapter 3. Basic Wave Dynamics

3.1 Introduction

- There are 2 types of waves:

  (1) Mechanical waves: A physical restoring force and a medium for propagation are the two fundamental elements of all wave motion in solids, liquids, and gases.
  Examples: atmospheric waves, oceanic waves, sound (acoustic) waves, wind-induced waves, seismic waves, or even traffic density waves.

  (2) Electromagnetic waves: Electromagnetic waves do not require a medium. Instead, they consist of periodic oscillations of electrical and magnetic fields generated by charged particles and can therefore travel through a vacuum.
  Examples: radio waves, microwaves, infrared radiation, visible light, ultraviolet radiation, X-rays, and gamma rays.

- When an air parcel is displaced from its initial position, a *restoring force* may cause it to return to its initial position. In doing so, inertia will cause the air parcel to overshoot and pass its initial equilibrium position moving in the opposite direction from that in which it is initially displaced, thereby creating an oscillation around the equilibrium position.

Concurrently, a wave is produced that propagates from this source region to another part of the fluid system, which is the physical *medium of wave propagation*.

- Thus, a physical restoring force and a medium for propagation are the two fundamental elements of all wave motion in solids, liquids, and gases, including atmospheric waves, oceanic waves, sound (acoustic) waves, wind-induced waves, seismic waves, or even traffic density waves.
- The ultimate behavior of the wave is dictated by the individual properties of the restoring force responsible for wave generation and the medium through and by which the wave propagates energy and momentum.
- Waves are everywhere!
- Note that waves are different from mass transportation, such as outflow from a thunderstorm out and density current below it.

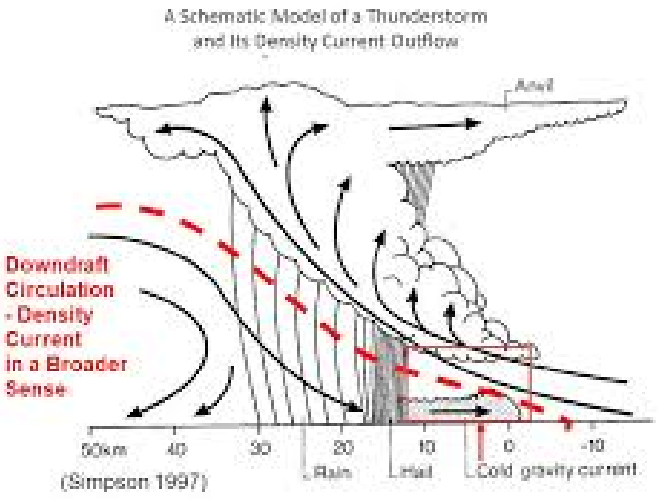

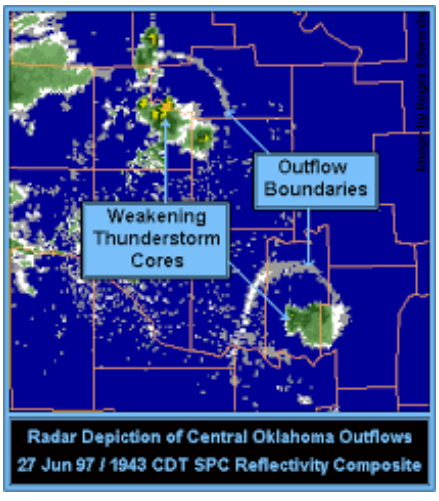

- Atmospheric waves may be classified as follows (Table 3.1): (a) sound (acoustic) waves, (b) mesoscale waves, and (c) planetary (Rossby) waves.

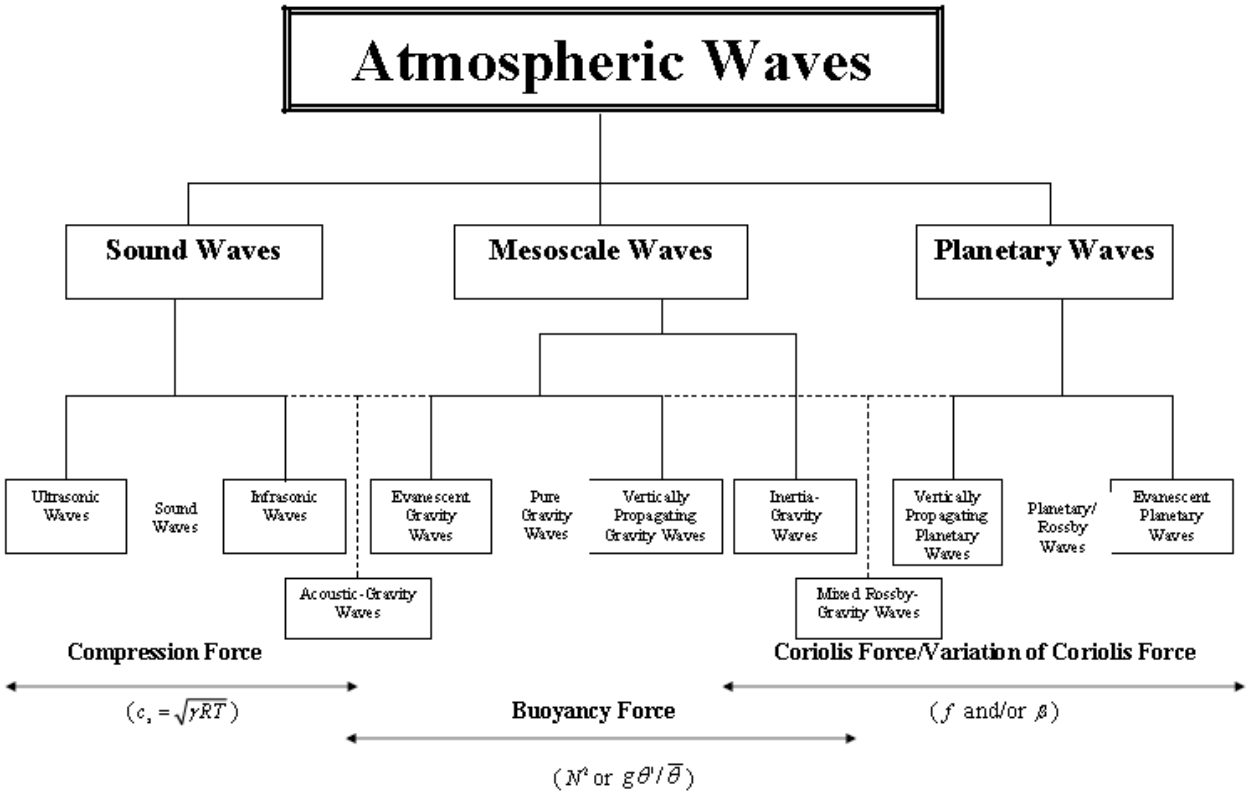

Table 3.1 (Lin 2007)

- In this lecture, mesoscale waves are defined in a more general manner, referring to waves that exist and propagate in the atmosphere with a mesoscale wavelength.

  Thus, mesoscale waves include pure gravity waves and inertia-gravity waves. A more detailed classification of these waves and their probable restoring or wave generation forces are summarized in Table 3.1.

- Each group of waves exhibits multiple wave regimes. For example, as will be discussed later, pure gravity waves may be further categorized as either vertically propagating waves or evanescent waves, depending upon whether the wave energy is free to propagate vertically.

- The restoring forces for pure gravity waves and inertia oscillations are the buoyancy force ($-g\rho'/\bar{\rho}$ or $g\theta'/\bar{\theta}$) and Coriolis force, respectively.

- Sound waves derive their oscillations from longitudinal compression and expansion. Longitudinal wave means that the wave propagates in the same direction as the oscillation.

- Planetary waves derive their oscillations from the meridional variation of the Coriolis force or β effect due to the conservation of angular momentum. Planetary waves are also called Rossby waves.

- The compression force, buoyancy force, Coriolis force, and variation of Coriolis forces in the atmosphere are often shown in governing equations, respectively by c_s, N^2 $(= \frac{g}{\theta}\frac{\partial \theta}{\partial z})$, f, and β in governing equations.

- Restoring forces may also combine and work together to generate mixed waves, such as inertia-gravity waves, mixed acoustic-gravity waves, and mixed Rossby-gravity waves.

- Inertia-gravity waves are also known as Poincaré waves on the ocean or water surface and as coastal or boundary Kelvin waves along a rigid, lateral boundary such as a shoreline or coast.

- The oscillation period of the waves is determined by the strength of the restoring force and characteristics in the wave medium.

- The presence of mesoscale waves in the atmosphere and oceans can be measured and inferred from (a) thermodynamic soundings, (b) microbarograph pressure traces, (c) visible and infrared satellite images, (d) radar echoes, (e) sodar, (f) rawinsonde, (g) vertical wind profilers, etc.

  Data obtained from these sources and instruments may be used to help predict mesoscale wave generation and propagation, as well as to help explain the development and subsequent evolution of a variety of mesoscale scale weather phenomena associated with the passage of these waves.

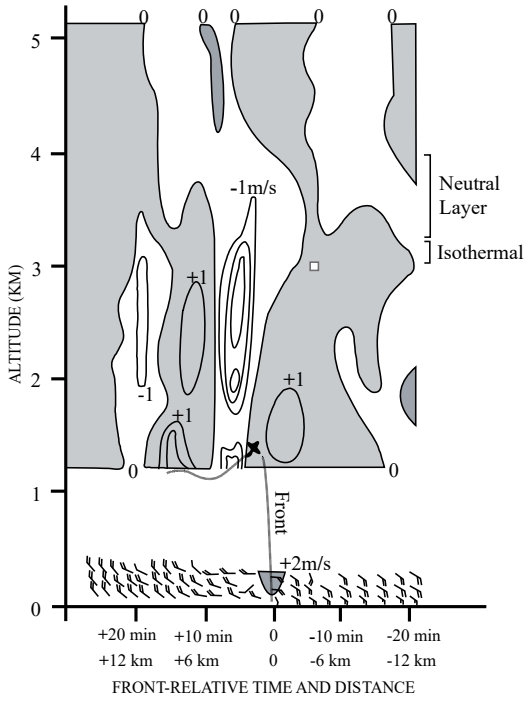

Fig. 4.2: An example of gravity waves generated by a density current, as revealed by a synthesis of sodar, rawinsonde, and wind profiler observations during the Mesogers field experiment in southwestern France. (From Ralph et al. 1993; Lin 2007)

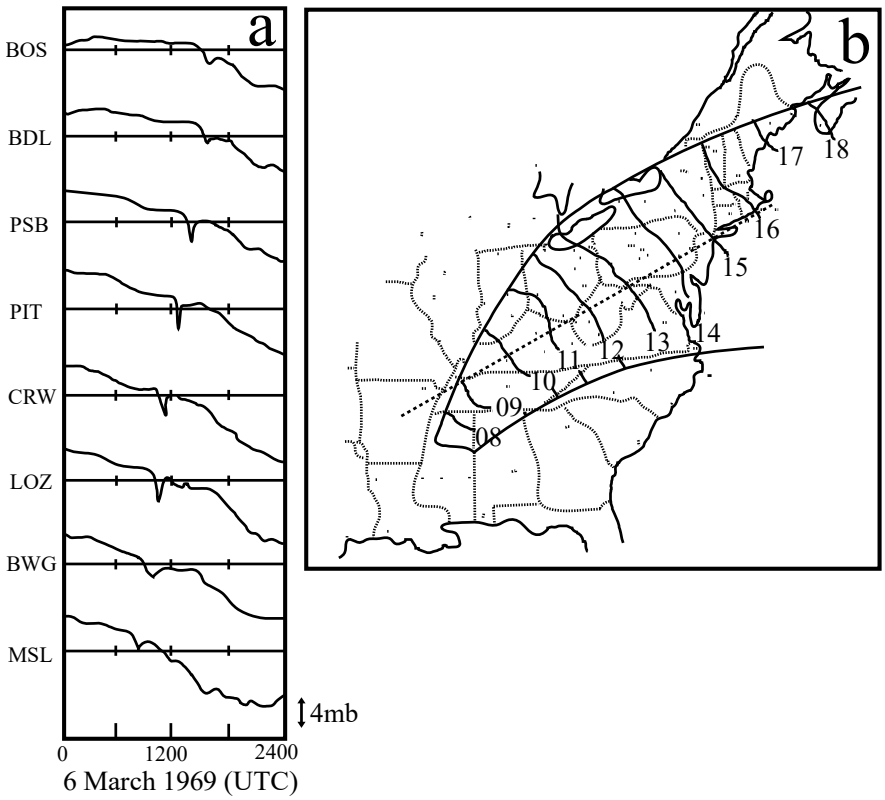

Fig. 4.5: (a) Surface pressure traces for selected stations on 6 March 1969: (1) BOS - Boston, MA; (2) BDL – Hartford, CT, (3) PSB – Philipsburg; (4) PIT – Pittsburgh; (5) CRW – Charleston, WV; and (6) LOZ – London, KY, (7) BWG - Bowling Green, KY; MSL – Muscle Shoals, AL. (b) Isochrones (hours in UTC) of the minimum pressure indicating passage of the solitary wave. The heavy dashed line indicates the position of the sounding cross section shown in Fig. 4.17b, as well as the primary direction of travel of the wave. (From Lin and Goff 1988)

Fig. 7.9: Kelvin-Helmholtz billow clouds (p. 253-254, Lin 2007)

1972 Boulder Severe Downslope Windstorm

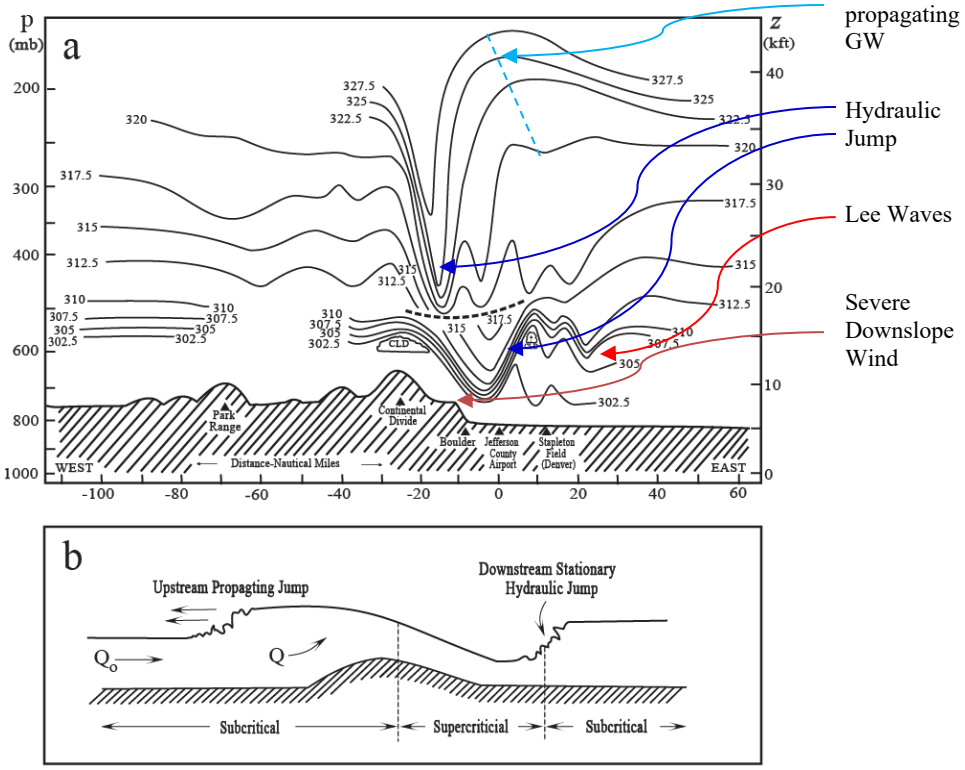

Lee waves

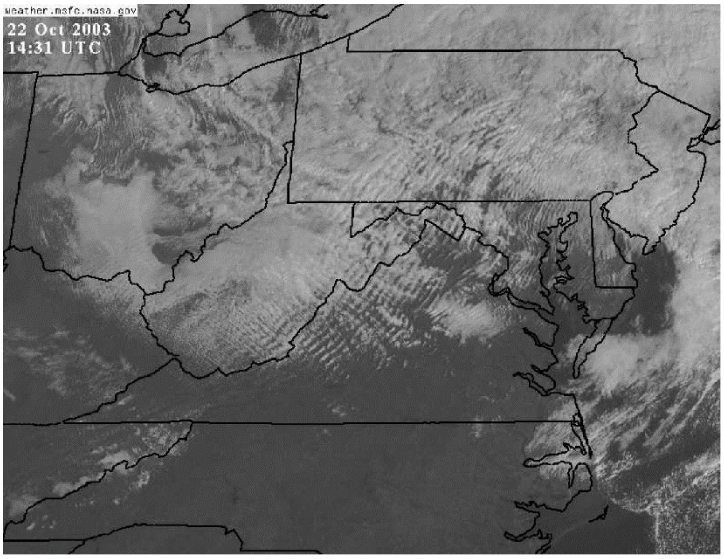

- In previous studies of large-scale dynamics and numerical weather prediction (NWP), mesoscale and sound waves were often regarded as undesirable "noise".

  The reason is that they often appear as small perturbations or disturbances embedded in the large-scale flow, and their presence can even trigger numerical instabilities in an operational forecast model if the grid interval of the NWP model is not sufficiently small.

  Therefore, they are often filtered out from the primitive equations in the NWP models.

- However, mesoscale waves do have major dynamical impacts on the atmosphere and cannot be simply removed from the NWP models, such as:

  (a) The initiation of severe convective storms and the organization of individual convective cells or elements into larger-scale convective systems.
  (b) The spectral transfer of energy between large and small-scale motions.
  (c) The vertical and horizontal transport of energy and momentum from one region of the atmosphere to another.
  (d) The generation of disturbances, such as mountain waves and clear-air turbulence (CAT), that can adversely affect airflow, weather, and aviation safety etc.
  (e) The triggering of hydrodynamic instabilities that lead to the generation of severe weather.

- To understand the above-mentioned atmospheric processes and better predict them, it is essential to understand the dynamics of mesoscale waves.

- In this chapter (Ch. 3 of Lin 2007), we will derive the governing equations and dispersion relationships for mesoscale waves, based on linearized equations derived from perturbation theory, and then discuss wave properties for different flow regimes.

- Since linear wave theory provides a powerful tool that helps to analyze and predict the variety of mesoscale waves observed in the atmosphere and those predicted by numerical models, we will restrict ourselves to this mathematical framework almost exclusively.

- To help understand basic wave properties, we will begin the discussion with sound waves and shallow water waves.

- In a structured atmosphere, mesoscale waves, just as synoptic or planetary-scale waves, may be reflected, transmitted, and even over-reflected from certain internal boundaries. These properties will be discussed in the later lecture notes.

3.2 Basic Wave Properties

- With the Boussinesq approximation, the linearized perturbation equations, (2.2.14) – (2.2.18), can be combined into a single equation for the vertical velocity *w'*,

$$\frac{D}{Dt}\left\{\frac{D^2}{Dt^2}\nabla^2 w' + f^2 w'_{zz} - \left(U_{zz}\frac{D}{Dt} + fV_{zz}\right)w'_x - \left(V_{zz}\frac{D}{Dt} - fU_{zz}\right)w'_y + N^2\nabla_H^2 w' + 2f\left(U_z w'_{yz} - V_z w'_{xz}\right)\right\}$$
$$+2fU_zV_z\left(w'_{xx} - w'_{yy}\right) + 2f\left(V_z^2 - U_z^2\right)w'_{xy} - 2f^2\left(U_z w'_{xz} + V_z w'_{yz}\right) = \frac{g}{c_p T_o}\frac{D}{Dt}\nabla_H^2 q', \tag{3.2.1}$$

where $D/Dt = \partial/\partial t + U\partial/\partial x + V\partial/\partial y$.

- The above equation governs the small-amplitude vertical velocity *w'* in a mesoscale system, which may contain the following mechanisms:

  (a) pure gravity and inertia-gravity wave generation
  (b) static instability
  (c) Kelvin-Helmholtz (shear) instability
  (d) symmetric instability
  (e) baroclinic instability.

- For different flow regimes, the Boussinesq form of (2.2.14) - (2.2.18) may reduce to different approximate equations, which will be further discussed in Sections 3.5 and 3.6 of Lin (2007).

- In addition to restoring forces and propagation media, wave motions may be characterized by several fundamental properties, such as wave frequency, wave number, phase speed, group velocity, and dispersion relationship, which will be discussed below.

Note that the *dispersion relationship relates the wave frequency to the wave number*.

- Wave properties

  oscillation period: τ

  wave frequency: $\omega = 1/\tau$ (i.e., what you learned in general physics)

  angular wave frequency: $\omega = 2\pi/\tau$

  horizontal and vertical spatial scales: L_x, L_y, L_z

  horizontal and vertical wave numbers: $k = 1/L_x$, $l = 1/L_y$, $m = 1/L_z$

  angular wave numbers: $k = 2\pi/L_x$, $l = 2\pi/L_y$, $m = 2\pi/L_z$

- A wave may be characterized by its amplitude and phase,

$$\varphi = \text{Re}\ \{A \exp[i(kx + ly + mz - \omega t - \alpha)]\}$$

  where

  φ : any of dependent flow variable (e.g., u, v, w, p, T, ρ)

  Re: real part

  A : amplitude

  $kx + ly + mz - \omega t - \alpha$: phase

  α : phase angle. The phase angle is determined by the initial position of the wave.

- Lines of constant phase, such as wave crests, troughs, or any other particular part of the wave propagate through the fluid medium at a speed called the phase speed.

  Phase speeds in x, y, and z directions, are respectively given by

$$c_{px} = \omega/k; \quad c_{py} = \omega/l; \quad \text{and} \quad c_{pz} = \omega/m \qquad (3.2.2)$$

  e.g. Look at $u(x, t) = u_o \sin(kx - \omega t)$, constant phase: $kx - \omega t = 0$.

- If an observed or experimental set of data is available, the phase speed of a wave may be estimated by determining and tracing a constant phase of the wave.

- In a geophysical fluid system such as the atmosphere, waves normally are very complicated in form, due to the superposition of wave components with different wavelengths and their nonlinear interactions, and cannot be represented by a simple, single sinusoidal wave.

- However, a small-amplitude wave with any shape can be approximately represented by a linear superposition of wave trains of different wave numbers, i.e. a Fourier series of sinusoidal components.

- For example, a wave in the x direction may be decomposed into sinusoidal components of the form,

$$\varphi(x) = \sum_{n=1}^{\infty} \left(A_n \sin k_n x + B_n \cos k_n x \right), \tag{3.2.3}$$

where the Fourier coefficients A_n and B_n are determined by

$$A_n = \frac{2}{L} \int_0^L \varphi(x) sin \frac{2\pi n x}{L} dx \,, \tag{3.2.4}$$

$$B_n = \frac{2}{L} \int_0^L \varphi(x) cos \frac{2\pi n x}{L} dx \,. \tag{3.2.5}$$

The nth Fourier component or nth harmonic of the wave function φ_n is defined as $\varphi_n = A_n \sin k_n x + B_n \cos k_n x$.

- In deriving (3.2.4) and (3.2.5), we have used the orthogonality relationships,

$$\int_0^L \sin\frac{2\pi nx}{L}\cos\frac{2\pi mx}{L}dx = 0, \qquad \text{for all } n, m > 0\ ,$$

$$\int_0^L \sin\frac{2\pi\, nx}{L}\sin\frac{2\pi\, mx}{L}dx = \begin{Bmatrix} 0, & n \neq m \\ L/2, & n = m \end{Bmatrix}, \text{ and}$$

$$\int_0^L \cos\frac{2\pi\, nx}{L}\cos\frac{2\pi\, mx}{L}dx = \begin{Bmatrix} 0, & n \neq m \\ L/2, & n = m \end{Bmatrix}. \qquad (3.2.6)$$

- If a wave is composed of a series of Fourier components of different wavelengths, then the phase speed for each individual component may also be different, according to (3.2.2).

- If the phase speed is independent of wave number or wavelength, then the wave will retain its initial shape and remain coherent as it propagates throughout the fluid medium. This type of wave is *nondispersive*.

- On the other hand, if the phase speed is a function of wave number or wavelength, then the wave will not be able to retain its initial shape and remain coherent as it propagates in the medium since each Fourier component is propagating at a different phase speed. In other words, the wave is *dispersive*.

- Thus, it becomes clear that the relationship between wave frequency and wave number determines whether the wave is dispersive.

- Although visually, a dispersive wave may look like it is dissipative, dispersion and dissipation are completely different physical processes.

- In a dissipative, but nondispersive wave, every Fourier component of the wave propagates at the same speed, while the wave amplitude decreases. Thus, individual wave groups preserve their phase (shape) during propagation.

- If the wave is nondispersive, then the wave pattern moves throughout the medium without any change in shape of the initial waveform. This means that the *phase velocity* of the individual wave crests (c_p) is equal to the *group velocity* of the slow-varying modulations or the envelope of Fourier wave components (c_g).

- In summary, a wave is nondispersive if:
  (a) Phase velocity of the wave is independent of wave number, i.e. $c_p \neq f(k)$ ($c_{px} \neq f(k); c_{py} \neq f(l); c_{pz} \neq f(m)$ for 3D wave), or
  (b) Phase velocity equals to group velocity ($c_g = c_p$). Otherwise, the waves are dispersive.

The concept of group velocity is illustrated in Fig. 3.1.

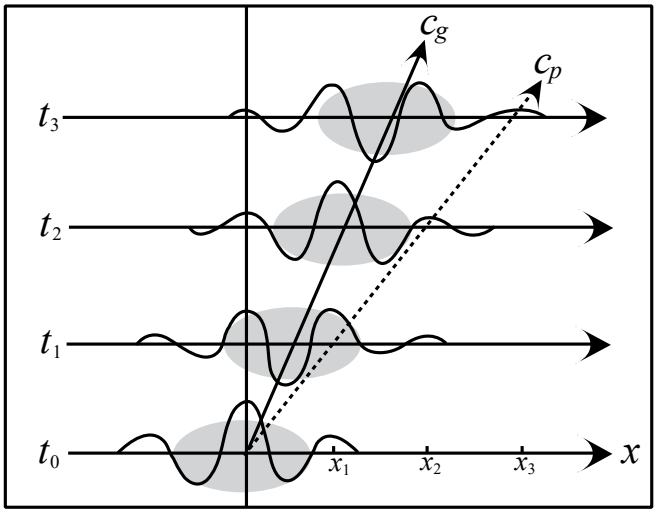

Fig. 3.1: Propagation of a wave group and an individual wave. The solid and dashed lines denote the group velocity (c_g) and phase velocity (c_p), respectively. Shaded oval denotes the concentration of wave energy which propagates with the group velocity. The phase speed c_p equals x_i / t_i, where i = 1, 2, or 3.

In Fig. 3.1, the simple group of two superimposed sinusoidal waves, represented by the wave function

$$\varphi = \mathrm{Re}\{A\exp[i((k+\Delta k)x-(\omega+\Delta\omega)t)]+A\exp[i((k-\Delta k)x-(\omega-\Delta\omega)t)]\}$$

propagates at the speed $\Delta\omega/\Delta k$.

This velocity approaches $\partial\omega/\partial k$ as $\Delta k \to 0$, which is defined as the group velocity (in the x direction). In other words, $c_g = \partial\omega/\partial k$.

Thus, the group velocity represents the velocity the slow-varying modulation of a wave propagates. For 3D waves, the group velocity is given by

$$\boldsymbol{c_g} = c_{gx}\boldsymbol{i} + c_{gy}\boldsymbol{j} + c_{gz}\boldsymbol{k} = \frac{\partial\omega}{\partial k}\boldsymbol{i} + \frac{\partial\omega}{\partial l}\boldsymbol{j} + \frac{\partial\omega}{\partial m}\boldsymbol{k}\,. \qquad (3.2.7)$$

- Transverse waves

  When a wave propagates in the direction perpendicular to the wave motion, the wave is called transverse wave.

  For example, the incompressible continuity equation, one can show that

  $$\boldsymbol{k}\cdot\boldsymbol{V}' = 0\,, \qquad (3.2.8)$$

  where $\boldsymbol{k} = (k, l, m)$ is the *wave number vector*.

  For two-dimensional plane waves (e.g., $l = 0$), the above equation indicates that the wave motion or oscillation of fluid parcels is perpendicular to the wave number vector.

➢ Wave front

At any instant t_o, a *wave front* is defined by setting the phase ($\boldsymbol{k}\cdot\boldsymbol{x}-\omega t$ - α) to be constant, which indicates that a family of parallel planes is normal to the wave number vector $\boldsymbol{k}$. As time proceeds, these planes move with the phase speed in the direction $\boldsymbol{k}$. Notice that the phase velocity can be derived as

$$\boldsymbol{c}=\omega\boldsymbol{k}/k^2 . \tag{3.2.9}$$

That is, the phase velocity $\boldsymbol{c}$ is parallel to $\boldsymbol{k}$. As will be discussed in Section 3.6, inertia-gravity waves are an example of *transverse waves* because the fluid particle motion, $\boldsymbol{V}'$, is perpendicular to the phase velocity (Fig. 3.9 or Fig. 3.10a), as indicated by (3.2.8). Note that the phase speeds in the x and z directions do not comprise the phase velocity. That is,

$$\boldsymbol{c}\neq(\omega/k,\omega/l,\omega/m) . \tag{3.2.10}$$

For sound waves (Section 3.3), it can be shown that

$$\boldsymbol{k}\cdot\boldsymbol{V}'\neq 0 . \tag{3.2.11}$$

This means the wave propagates in the same direction as the wave motion. This type of waves is called longitudinal wave. Thus, sound waves are an example of *longitudinal waves*.

In the following, we will discuss about a simple fluid flow system, such as a shallow water system, which will help us understand the gravity wave dynamics.

3.3 Sound Waves

➢ Sound (acoustic) waves derive their oscillations from the compression and expansion of the medium due to the compression force.

Let us consider one-dimensional ($\partial/\partial y = \partial/\partial z = 0$), small-amplitude, adiabatic perturbations in a non-rotating, inviscid, uniform (no basic wind shear) flow governed by (2.2.14) – (2.2.18),

$$\frac{\partial u'}{\partial t} + U\frac{\partial u'}{\partial x} + \frac{1}{\overline{\rho}}\frac{\partial p'}{\partial x} = 0, \tag{3.3.1}$$

$$\frac{\partial p'}{\partial t} + U\frac{\partial p'}{\partial x} + \gamma\overline{p}\frac{\partial u'}{\partial x} = 0. \tag{3.3.2}$$

In Eq. (3.3.2), $\gamma = c_p / c_v$. The above two equations may be combined into a single equation for *p'*,

$$\left(\frac{\partial}{\partial t} + U\frac{\partial}{\partial x}\right)^2 p' - c_s^2\frac{\partial^2 p'}{\partial x^2} = 0, \tag{3.3.3}$$

where c_s is the sound (acoustic) wave speed, which is defined as

$c_s = \sqrt{\gamma R\overline{T}}$.

Assuming a wave-like solution,

$$p(x,t) = p_o e^{i(kx-\omega t)} = p_o[\cos(kx-\omega t) + i\sin(kx-\omega t)],$$

and substituting it into (3.3.3) leads to

$$\omega = (U \pm c_s)k. \tag{3.3.4}$$

For brevity, we omit the Re{ } notation (real part) in the wave-like solution, but it is to be understood that only the real part of the above solution has physical significance.

The above method of the assumption of wave-like solutions for the small-amplitude perturbations is also referred to as the *method of normal modes*.

The above equation is the dispersion relation for sound waves, which relates the wave frequency ω to the horizontal wave number k.

From (3.3.4), we may obtain the horizontal phase speeds, which are given by

$$c_p = \frac{\omega}{k} = U \pm c_s . \tag{3.3.5}$$

Eq. (3.3.5) represents phase speeds of the downstream ($U + c_s$) and upstream ($U - c_s$) propagating sound waves, which are simultaneously being advected by the basic wind U.

Sound waves are nondispersive since their phase speeds are independent of wave number. This nondispersive property of sound waves may also be verified by showing that the group velocities for these waves c_g are identical to their phase speeds c_p.

- Consider a semi-infinite tube filled with gas whose right-hand side extends to infinity and whose left-hand side is confined by a piston.

When the gas is alternatively compressed and expanded by oscillating the piston in and out of the left hand side of the semi-infinite tube, an air parcel located adjacent to the piston will be forced to oscillate back and forth about its equilibrium position due to the oscillating horizontal pressure gradient and, concurrently, a sound wave will be excited that propagates toward the right at the speed $c_s = \sqrt{\gamma R \overline{T}}$.

In a dry, isothermal atmosphere with a constant temperature of 300 K, a one-dimensional acoustic wave has a phase speed and group velocity of approximately 347 ms^{-1} (~ 776 mph).

- In fact, the general solution of (3.3.3) may be written as,

$$p' = F[x + (U + c_s)t] + F[x + (U - c_s)t], \qquad (3.3.6)$$

where F is any arbitrary function whose amplitude is one-half that of the initial disturbance, and whose shape is identical to that of the initial disturbance.

In a quiescent fluid, the first and second terms on the right hand side of (3.3.6) represent the leftward and rightward propagating sound waves, respectively.

Since sound waves do not play significant dynamic roles in affecting most atmospheric motions, they are often eliminated from the primitive equations - particularly those that are commonly employed in most current operational NWP models.

Although sound waves may have no particular relevance to atmospheric motions in the troposphere that are responsible for "weather", a special class of waves called *Lamb waves* has been observed. These waves can propagate horizontally in an isothermal atmosphere in the absence of vertical motion. Lamb waves, as well as sound waves and gravity waves, can be generated by latent heat release in a convective storm (e.g., Nicholls and Pielke 2000).

In a two-dimensional, i.e. in (x, z) vertical plane ($\partial/\partial x \neq 0,\ \partial/\partial z,\ \partial/\partial y = 0$), adiabatic, hydrostatic, non-rotating, inviscid,

isothermal atmosphere with no vertical motion and basic wind shear, small-amplitude motions are governed by (2.2.14) – (2.2.18) reduced to (3.3.1), (3.3.2), and

$$\frac{1}{\bar{\rho}}\left(\frac{\partial p'}{\partial z}+\frac{p'}{H}\right)=g\frac{\theta'}{\bar{\theta}}, \tag{3.3.7}$$

$$\frac{\partial \theta'}{\partial t}+U\frac{\partial \theta'}{\partial x}=0. \tag{3.3.8}$$

Note that in an isothermal atmosphere, the scale height, $H=c_s^2/g$, is a constant. Equations (3.3.7) and (3.3.8) may be combined to yield an equation that, when coupled with (3.3.3), forms the set of equations governing the evolution of Lamb waves.

3.4 Shallow Water Waves

- Consider a
  (1) non-rotating,
  (2) hydrostatic,
  (3) two-layer fluid system with constant densities ρ_1 and ρ_o in the upper and lower layers, respectively, (Fig. 3.2) and
  (4) $\rho_1 < \rho_o$, the pressure gradients at the interface can be approximated by

$$\frac{\partial p}{\partial x}=g\Delta\rho\frac{\partial(h+h_s)}{\partial x},$$

$$\frac{\partial p}{\partial y}=g\Delta\rho\frac{\partial(h+h_s)}{\partial y},$$

where $\Delta\rho=\rho_o-\rho_1$ and h_S is the height of the topography (see Fig. 3.2). In deriving the above equations, we have used $h+h_S=H+h'$, where h is the depth of the fluid.

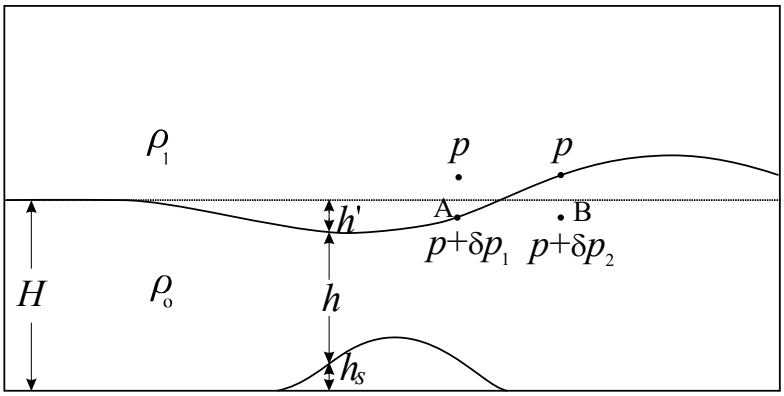

Fig. 3.2: A two-layer system of homogeneous fluids. Symbols H, h, h_s, and h' denote the undisturbed fluid depth, actual fluid depth, bottom topography, and perturbation (vertical displacement) from the undisturbed fluid depth, respectively. The densities of the upper and lower layers are ρ_1 and ρ_o, respectively. The pressure perturbations at A and B from p in the upper layer are denoted by $p+\delta p_1$ and $p+\delta p_2$, respectively.

- By assuming no initial vertical shear, the horizontal momentum equations become

$$\frac{\partial u}{\partial t}+u\frac{\partial u}{\partial x}+v\frac{\partial u}{\partial y}=-g'\frac{\partial(h+h_s)}{\partial x}, \tag{3.4.1}$$

$$\frac{\partial v}{\partial t}+u\frac{\partial v}{\partial x}+v\frac{\partial v}{\partial y}=-g'\frac{\partial(h+h_s)}{\partial y}, \tag{3.4.2}$$

where $g'=g\Delta\rho/\rho_o$ is the *reduced gravity*.

- The continuity equation in a shallow water system can be derived,

$$\frac{\partial h}{\partial t}+u\frac{\partial h}{\partial x}+v\frac{\partial h}{\partial y}+h\left(\frac{\partial u}{\partial x}+\frac{\partial v}{\partial y}\right)=0, \tag{3.4.3}$$

One may substitute $u=U+u'$, $v=V+v'$, and $h=H+h'-h_s$ to obtain the perturbation form,

$$\frac{\partial u'}{\partial t}+(U+u')\frac{\partial u'}{\partial x}+(V+v')\frac{\partial u'}{\partial y}+g'\frac{\partial h'}{\partial x}=0, \tag{3.4.4}$$

$$\frac{\partial v'}{\partial t}+(U+u')\frac{\partial v'}{\partial x}+(V+v')\frac{\partial v'}{\partial y}+g'\frac{\partial h'}{\partial y}=0 \tag{3.4.5}$$

$$\frac{\partial h'}{\partial t}+(U+u')\frac{\partial h'}{\partial x}+(V+v')\frac{\partial h'}{\partial y}+(H+h'-h_s)\left(\frac{\partial u'}{\partial x}+\frac{\partial v'}{\partial y}\right)=(U+u')\frac{\partial h_s}{\partial x}+(V+v')\frac{\partial h_s}{\partial y}. \tag{3.4.6}$$

➢ Special Case - 2D, linear, one-layer system

The governing equations for two-dimensional, small-perturbation (linear), one-layered fluid system with a flat bottom reduce to the following

$$\frac{\partial u'}{\partial t}+U\frac{\partial u'}{\partial x}+g'\frac{\partial h'}{\partial x}=0\,, \tag{3.4.7)'}$$

$$\frac{\partial h'}{\partial t}+U\frac{\partial h'}{\partial x}+H\frac{\partial u'}{\partial x}=0. \tag{3.4.8)'}$$

The above two equations may be combined to

$$\left(\frac{\partial}{\partial t}+U\frac{\partial}{\partial x}\right)^2 h'-(gH)\left(\frac{\partial^2 h'}{\partial x^2}\right)=0\,. \tag{3.4.9)'}$$

We may obtain the solution directly from the governing equation,

$$h'(t,x)=\frac{1}{2}f\left(x+\left(U+\sqrt{gH}\right)t\right)+\frac{1}{2}f\left[x+\left(U-\sqrt{gH}\right)t\right], \tag{3.4.12)'}$$

where *f* preserves the same shape of the initial disturbance but with the amplitude reduced to half. For example, the shallow-water waves with the initial disturbance

$$h'(x)=\frac{h_o b^2}{x^2+b^2}\,, \tag{3.4.13}$$

are represented by,

$$h'(x,t)=\frac{(h_o/2)b^2}{\left[x+\left(U+\sqrt{gH}\right)t\right]^2+b^2}+\frac{(h_o/2)b^2}{\left[x+\left(U-\sqrt{gH}\right)t\right]^2+b^2}\,. \tag{3.4.14}$$

- The governing equation for a two-dimensional, small-perturbation shallow water fluid flow over an obstacle can be derived,

$$\left(\frac{\partial}{\partial t}+U\frac{\partial}{\partial x}\right)^2 h' - (gH)\frac{\partial^2 h'}{\partial x^2} = U\left(\frac{\partial}{\partial t}+U\frac{\partial}{\partial x}\right)\frac{\partial h_s}{\partial x} \quad , \tag{3.4.16}$$

which gives the following steady state solution

$$h' = \left(\frac{U^2}{U^2 - gH}\right) h_s = \frac{h_s}{1 - F^{-2}} \quad ; \quad F \equiv \frac{U}{\sqrt{gH}} \tag{3.4.17}$$

where F is called the *Froude number*.

Thus, we have

$$h' \propto h_s \qquad \text{for } F > 1,$$

$$h' \propto -h_s \qquad \text{for } F < 1, \tag{3.4.18}$$

- Froude number is related to the ratio of KE and PE of the upstream, undisturbed basic flow.

Note that in the real atmosphere, ocean, or other geofluid, there is density variation with height (i.e., stratification). Thus, the Froude number is often defined as U/Nh in a stratified fluid flow, where N is the Brunt-Vaisala frequency and h is the mountain height.

Some scientists argued that the physical meaning of U/Nh is very different from the Froude number ($F \equiv U/\sqrt{gH}$), thus prefer to use Nh/U and called it nondimensional mountain height.

However, a recent study of Sun and Sun (2015, Geosci Lett.) shows that the Froude number defined as U/Nh can be interpreted in the same way as in a shallow-water fluid flow.

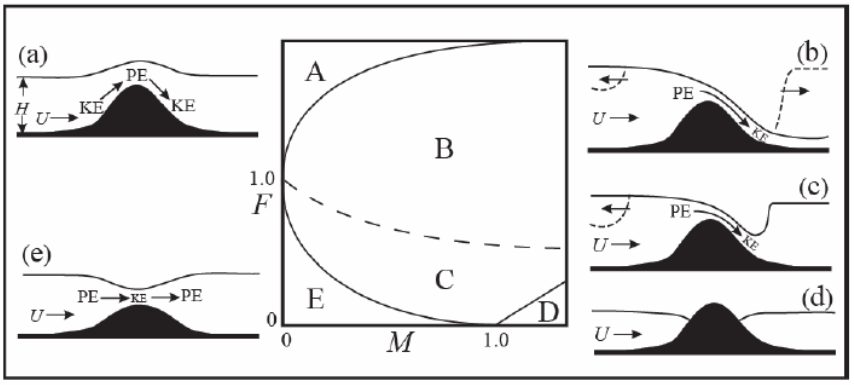

Fig. 3.3: Five flow regimes of the transient one-layer shallow water system, based on the two nondimensional control parameters ($F_o = U/\sqrt{gH}$, $M_c = h_m/H$): (a) supercritical flow, (b) flow with both upstream and downstream propagating jump, (c) flow with upstream propagating jump and downstream stationary jump, (d) completely blocked flow, and (e) subcritical flow. (Lin 2007; Adapted after Baines 1995 and Durran 1990)

(a) Supercritical Flow ($F > 1$)

If $F > 1$ far upstream, $h' \propto h_s$.

Thus, h' increases as $h_s(x)$ increases and the interface bows upwards over the obstacle (Fig. (3.3a)). Physically, this means that the upstream flow has enough kinetic energy to convert to potential energy and climb over the obstacle. This flow regime is called *supercritical flow*.

(e) Subcritical Flow ($F < 1$)

If $F < 1$, then $h' \propto -h_s$.

Thus, h' decreases as $h_s(x)$ increases.
Physically, this means that a fluid particle does not have enough kinetic energy to climb over the obstacle. In order to surmount the obstacle, the fluid particle needs to draw its potential energy to gain enough kinetic energy (Fig. 3.3e).

Over the peak of the obstacle, the fluid reaches its minimum speed. This flow regime is called *subcritical flow*. The square of F is the

ratio of the advection flow speed (U) to the shallow water wave or long wave speed ($\sqrt{gH}$).

Thus, when the flow is supercritical ($F > 1$), small disturbance cannot propagate upstream against the flow and any obstacle will produce a purely local disturbance.

When the flow is subcritical ($F<1$), shallow water (long) waves can propagate upstream. The steady state effect of this is to increase the layer depth upstream, i.e. increases the PE upstream, which then converts into KE when the fluid surmounts the obstacle. Thus, the fluid reaches its maximum speed over the mountain peak and the water surface dips down.

Note that in this type of "steady state" flow, we have

$$\frac{u'}{U} = -\left(\frac{1}{F^2}\right)\frac{h'}{H}\,. \qquad (3.4.19)$$

- Venturi effect: Pertubation fluid velocity (u') is proportional to the perturbation height (h'). For example, flow speeds up in a tube where it is narrower.

- Bernoulli effect: Venturi effect may be derived to obtain the Bermoull's equation if the continuity equation is involved.

$$\boxed{p + (1/2)\rho v^2 + \rho g h = const.}$$

- In a transient (unsteady) flow, more flow regimes may occur. Dividing Eq. (3.4.17)

$$h' = \left(\frac{U^2}{U^2 - gH} \right) h_s = \frac{h_s}{1 - F^{-2}} \;\; ; \;\; F \equiv \frac{U}{\sqrt{gH}} \qquad (3.4.17)$$

by H leads to another nondimensional control parameter, $M = h_m/H$, where M is also called nondimensional mountain height.

- Based on F and M, there exist 3 additional flow regimes (Figs. 3.3c-d), in a single-layer transient shallow water system (Long 1970, 1972; Houghton and Kasahara 1968).

(b) Flow with both upstream and downstream propagating jump (Fig. 3.3b)

As either F decreases or the non-dimensional obstacle height M increases, the upstream flow is partially blocked and the flow response shifts to the regime in which both an upstream *hydraulic jump* (*bore*) and a downstream jump form and propagate away from the obstacle as time proceeds (Regime b, Fig. 3.3b).

In this case, a transition from subcritical to supercritical states occurs over the peak of the obstacle. Very high velocities are produced along the lee slope since the potential energy associated with the upstream flow is converted to kinetic energy when the fluid passes over and descends along the lee slope of the obstacle.

Eventually, a steady state is established near the obstacle and the free surface shape acquires a *"waterfall-like" profile*.

(c) Flow with upstream propagating jump and stationary downstream jump (Fig. 3.3c)

As F decreases further, the flow shifts to the regime in which another upstream jump forms and propagates upstream, while the

downstream jump becomes stationary over the lee slope due to the weaker advection effect (Regime c, Fig. 3.3c).

Regimes b and c are characterized by high surface drag and large flow velocities on the lee slope and is referred to as the transitional flow. This transitional flow has been used to explain the formation of severe downslope windstorms in the atmosphere (e.g., Long, 1954; Smith, 1985; Durran, 1986; Bacmeister and Pierrehumbert, 1988).

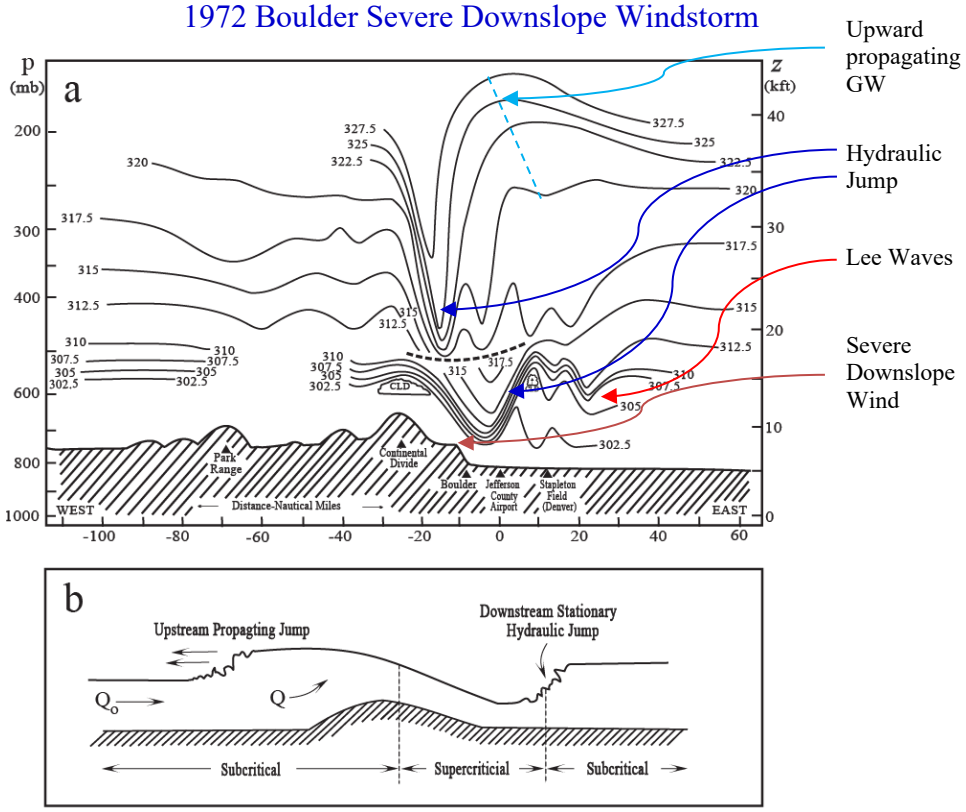

Fig. 3.4: (a) Analysis of potential temperature from aircraft flight data and rawinsondes for the 11 January 1972 Boulder *windstorm*. (b) A sketch of flow Regime C of Fig. 3.3(c), which may be used to explain the phenomenon associated with (a). Q is the volume flux per unit width. (Adapted after Turner 1973; Lin 2007)

- A severe downslope wind over the Front Range to the east of the continental divide reached a value of over 60 ms^{-1}. The mechanisms for producing severe downslope winds will be discussed in the chapter of orographically forced flow (Ch. 5). An example of an internal hydraulic jump occurred in the atmosphere is shown in Fig. 3.5.

Fig. 3.5: A hydraulic jump in a supercritical airflow over the Sierra Nevada mountain range, made visible by the formation of clouds, and by dust raised from the ground in the turbulent flow behind the jump. (Lin 2007; Photographed by Robert Symons, published in *Communication on Pure and Applied Math*, 20, no. 2, (review by M. J. Lighthill, @John Wiley and Sons, Inc., 1967).

(d) Completely blocked flow

With a very small F and $M > 1$, the flow response falls into the regime of *completely blocked flow* (Regime d in Fig. 3.3d).

- [Nonlinear Effects] If the nonlinear terms are considered, then *wave steepening* and *wave overturning* may occur.

The nonlinear effects on wave steepening may be elucidated by imaging an elevated wave, which is composed of several rectangular blocks with smaller blocks on top of larger blocks. Since the shallow water wave speed is proportional to the layer depth, the speed of fluid particles in the upper layer is higher than that in the lower layer. Thus, the wave front will steepen and possibly overturn. In the real atmosphere, once overturning occurs, the fluid becomes unstable and turbulence will be induced.

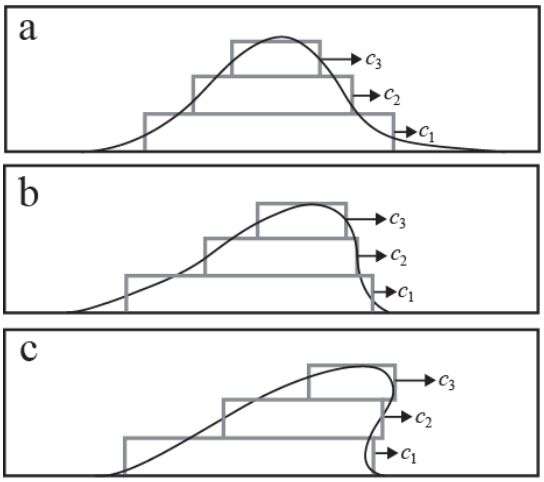

Fig. 3.6: The evolution of an initial symmetric wave, which is imagined to be composed of three rectangular blocks with shorter blocks on top of longer blocks. The wave speeds of these fluid blocks are approximately equal to $c_n = \sqrt{g(H+nh)}$, based on shallow-water theory, where n = 1, 2, and 3, H is the shallow-water layer depth, and h is the height of an individual fluid block. The wave steepening in (b) and wave overturning in (c) are interpreted by the different wave speeds of different fluid blocks because $c_3 > c_2 > c_1$.

- Note that for stratified fluid, the Froude number is defined differently, such as

$$F = \frac{U}{Nh}$$

It can be derived (Sun and Sun 2015, Geosci. Lett.) that the Froude number defined above is equivalent to that defined for shallow-water waves,

$$\mathrm{Fr} = \frac{U_i}{\sqrt{g'h}} = \frac{U_i}{\sqrt{g\frac{\theta'}{\theta}h}} = \frac{U_i}{\sqrt{gh\frac{\left(\theta_i\frac{d\bar{\theta}}{dz}h\right)-\theta_i}{\theta}}} = \frac{U_i}{\sqrt{\frac{g}{\theta}\frac{d\bar{\theta}}{dz}h^2}} = \frac{U_i}{Nh}. \qquad (21)$$

- Many flow characteristics found in shallow-water fluid flow are also shown in stratified fluid flow over mesoscale mountains.

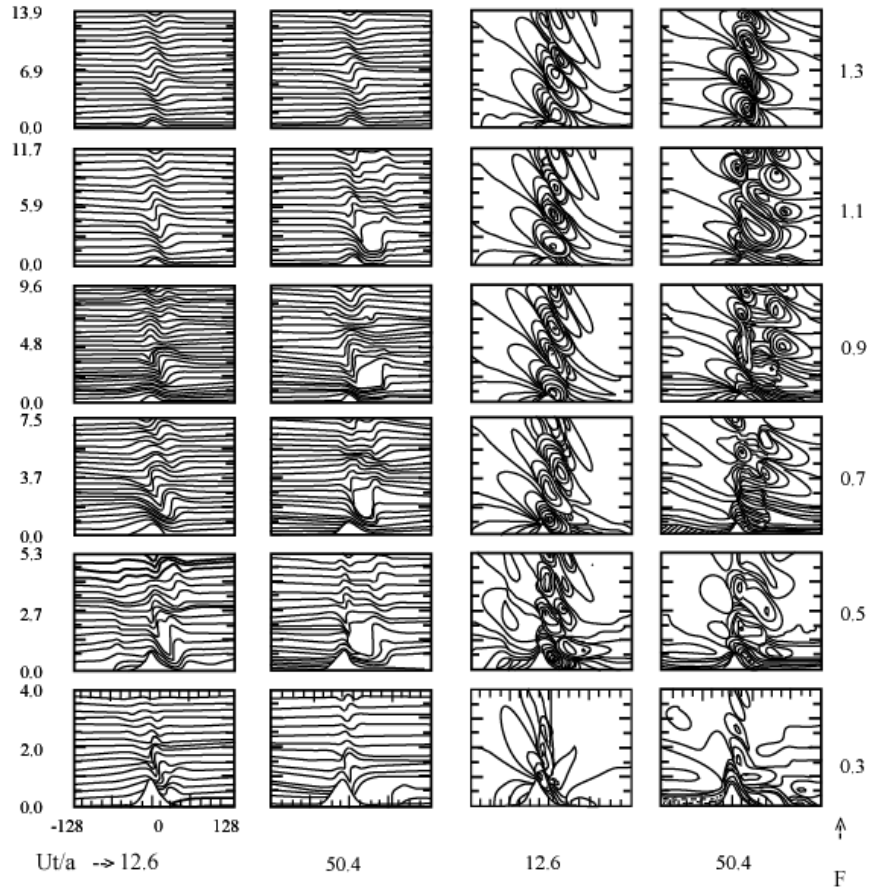

Fig. 6.10: Time evolution of the potential temperature fields (left two columns) and the horizontal velocity fields (right two columns) for a two-dimensional, hydrostatic, uniform flow over a bell-shaped mountain as simulated by a numerical model. (Lin 2007; Adapted from Lin and Wang, 1996)

Model Intercomparison for the 1972 Boulder Windstorm
(Mesoscale Alpine Programme-MAP; MAP & MAP D-Phase)

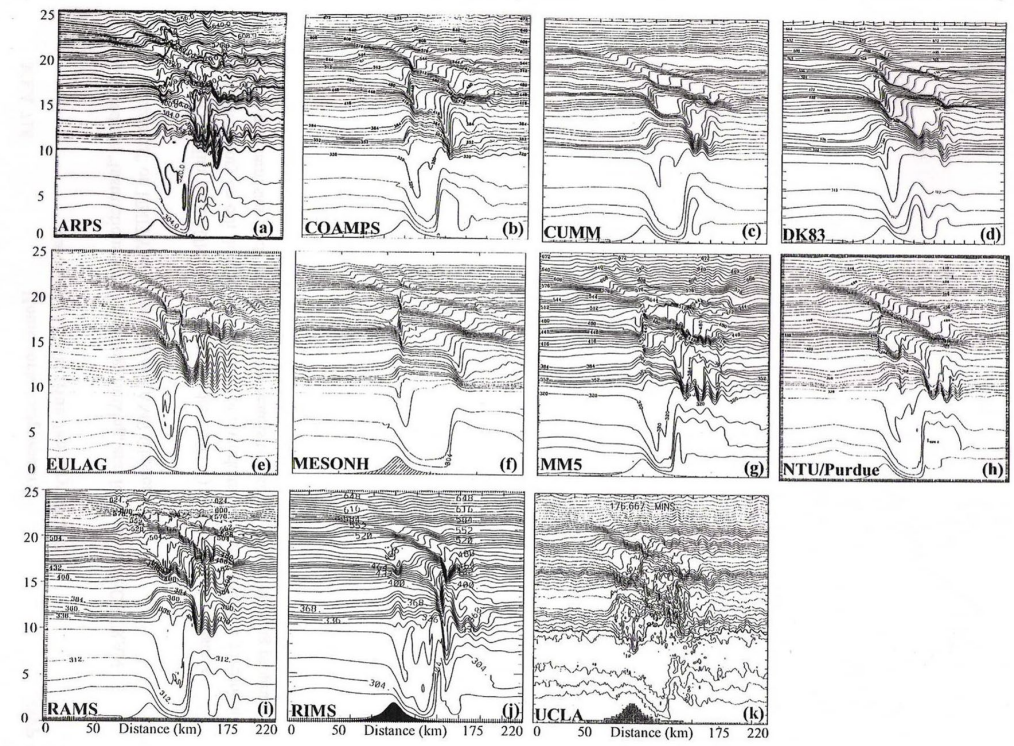

FIG. 3. Vertical cross section of the simulated potential temperature after 3 h for (a) ARPS, (b) COAMPS, (c) CUMM, (d) DK83, (e) EULAG, (f) MESO-NH, (g) MM5, (h) NTU/Purdue, (i) RAMS, (j) RIMS, and (k) UCLA models. The contour interval is 8 K.

(Doyle et al. 2000 MWR)

Model Intercomparison for the Terrain-Induced Rotor Experiment (T-Rex)

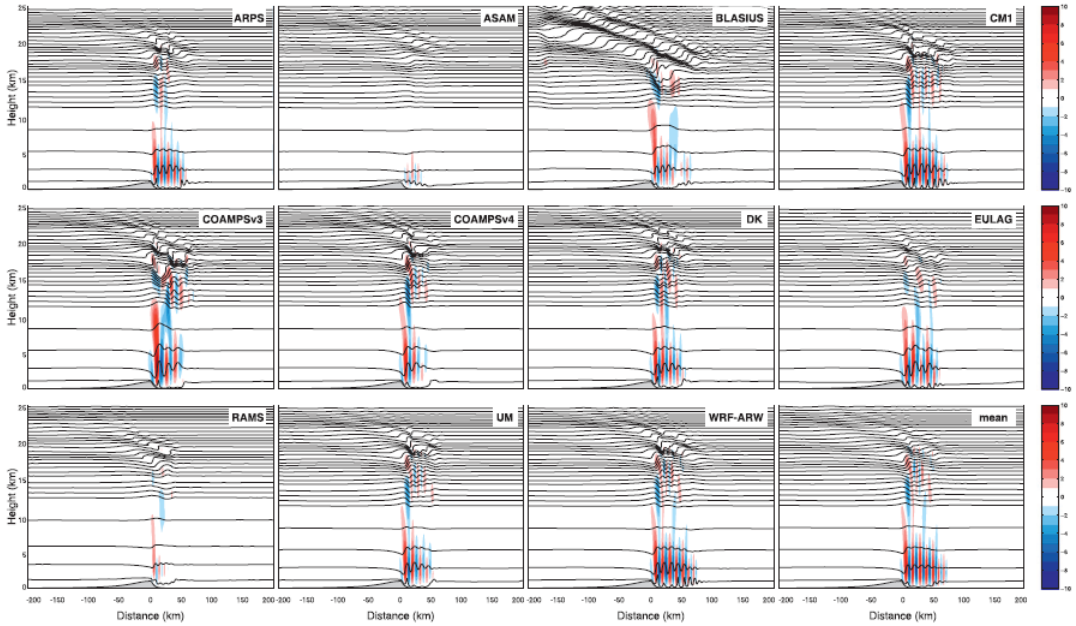

FIG. 4. Vertical velocity (color, interval 1 m s^{-1}) and potential temperature (black contours, interval 10 K) for Ex1000_fs case at the final time (4 h) for all models and (bottom right) the mean.

(Doyle et al., 2011, MWR)